AD-A244 104

MASTER COPY KEEP THIS COPY FOR REPRODUCTION PURPOSES

AD-A244 104

ON PAGE

Form Approved
OMB No. 0704-0188

Public gathe collect Davis I

je 1 hour per response, including the time for reviewing instructions, searching existing data sources, collection of information. Send comments regarding this burden estimate or any other aspect of this shington Headquarters Services, Directorate for Information Operations and Reports, 1215 Jefferson agement and Budget, Paperwork Reduction Project (0704-0188), Washington, DC 20503.

1. A	2. REPORT DATE 8/4/91	3. REPORT TYPE AND DATES COVERED Final 9/15/89 - 3/14/91

4. TITLE AND SUBTITLE
Measurements of Diffusion Rates of Liquids Through Materials

5. FUNDING NUMBERS
DAAL03-89-K-0165

6. AUTHOR(S)
P. M. Rentzepis

7. PERFORMING ORGANIZATION NAME(S) AND ADDRESS(ES)
Regents of the University of California
University of Califiornai, Irvine
Irvine, CA 92717

8. PERFORMING ORGANIZATION REPORT NUMBER

9. SPONSORING/MONITORING AGENCY NAME(S) AND ADDRESS(ES)
U. S. Army Research Office
P. O. Box 12211
Research Triangle Park, NC 27709-2211

10. SPONSORING/MONITORING AGENCY REPORT NUMBER
ARO 27550 3-CH-A

11. SUPPLEMENTARY NOTES
The view, opinions and/or findings contained in this report are those of the author(s) and should not be construed as an official Department of the Army position, policy, or decision, unless so designated by other documentation.

12a. DISTRIBUTION/AVAILABILITY STATEMENT
Approved for public release; distribution unlimited.

12b. DISTRIBUTION CODE

13. ABSTRACT *(Maximum 200 words)*

A simple experimental method was devised and built for the identification of very small trace quantities of molecules containing C=O and P=O functional groups. The system was tested successfully under laboratory conditions. The scientific papers have resulted from this work as of now.

92-00973

DTIC
ELECTE
JAN 10 1992
S D D

14. SUBJECT TERMS	15. NUMBER OF PAGES
Diffusion, Kinetics, Thermal Lensing	35
	16. PRICE CODE

17. SECURITY CLASSIFICATION OF REPORT	18. SECURITY CLASSIFICATION OF THIS PAGE	19. SECURITY CLASSIFICATION OF ABSTRACT	20. LIMITATION OF ABSTRACT
UNCLASSIFIED	UNCLASSIFIED	UNCLASSIFIED	UL

TABLE OF CONTENTS

Accesion For

NTIS CRA&I
DTIC TAB
Unannounced
Justification

By
Distribution /

Availability Codes

Dist | Avail and / or Special

A-1

Measurements of Diffusion Rates of Liquids Through Materials

Sponsored by The Army Resaerch Office
Contract No. DAAL03-89-K-0165

Grantee

The Regents of the University of California
University of California,irvine
Irvine, CA 92717

Final Report

Principal Investigator: Peter M. Rentzepis

Major findings.

We have discovered that we can detect nitrogen and phosphorous containing compounds by means of remote thermal lensing. Investigating the mechanism of photochemical reaction we find that the first intermediate is formed withing a few tenths of a picosecond while the formation and decay of the three subsequent intermediates are formed with rates varying from $3x10^{12}$ to $5x10^{8}$ sec. The ultrafast intermediates have being identified and the mechanism of rection established.

Measurement Diffusion Rates of Liquids through Materials

Contract # DAALO3-89-K-0165
Final Report

ABSTRACT

A simple experimental method was devised and built for the identification of very small trace quantities of molecules containing C=O and P=O functional groups. The system was tested successfully under laboratory conditions. Three scientific papers have resulted from this work as of now.

Introduction

The identification of molecular species is a very old problem which has been dealt adequately for samples in the solid, liquid and gas phases. Most analytical methods were performed *in situ* where a sample of the material to be analyzed is brought to the laboratory for analysis. Remote sensing is rather rare and more difficult to perform, especially at very low concentrations and in the case where the material must be distinguished form others of very similar structure. To achieve remote sensing of specific molecular structure we devised an experimental system and procedure which was based on thermal lensing and UV and Raman spectroscopy.

Thermal lensing techniques rely upon effect of heat generated as the absorbed light decays into vibrational modes of the medium thermal lensing and fluorescence have been utilized to determine fluorescent and non-fluorescent substances to a concentration of about 10^{-11} M. We believe that thermal lensing is an ideal method for the detection of trace amounts of chemical and biological agents because it is a strictly remote method, requiring no contact with any instruments or personnel, can be operated in closed or open terrain and has the sensitivity to detect and distinguish small amounts of closely related molecular species.

Experimental data suggest that this method and especially the special system to be constructed, has the potential to perform the functions of a very sensitive detector of minute traces of agents at remote distances.

Experimental

Thermal lensing is based upon the principle that light absorbed by a molecule will be dissipated, shortly, into its surrounding molecules, thus increasing the temperature. A temperature rise will result in the change of the index of refraction hence a lens will be formed in the sample due to the gradient in the temperature. The temperature gradient is caused by the Gaussian shape intensity distribution of the laser light which is used to excite the sample. The thermal lens generated is transient in nature and as dissipated with a rate controlled, to a large extent, by the thermal conductivity of the medium. Experimentally thermal lensing effects are measured as a relative change Δ the beam center intensity, I_{bc}, $\Delta I_{bc}/I_{bc}$ given by

$$\frac{\Delta I_{bc}}{I_{bc}} = \ln EA + \frac{\ln E^2 A^2}{2}$$

Where $E = P^*(dn/dt)/(1/91)\lambda k$

is the enhancement in sensitivity dn/dt the refractive index as a function of temperature, the wavelength k the thermal conductivity and A the absorbance at the sample at wavelength, and P the laser excitation power. It is possible to increase the $\frac{E}{P}$ signal by choosing materials which absorb highly, a laser light to coincide with the maximum absorption cross-section and solvents which show high $\frac{dn}{dt}$ and in the case of cw lasers low thermal conductivity.

The schematic diagram presented in figure 1 is a version of the most commonly used thermal lensing system. It consists of the pump laser in our case a Nd^{3t}/YAG cw mode locked laser, operated at 82 MHz, however a chopper has been inserted in the path between pump laser and the samples. The probe laser consists of a He/Ne laser collimated onto the sample and onto a photodetector which is coupled onto a computer and recorder via a lock-in amplifier. The strong pump laser pulses are prohibited from entering the detection system by a filter which stops the pump light, but allows the probe He/me beam to be transmitted. In our case, several more lengths were used which enabled us to excite either the electronic lenses located in

the UV or the vibrational levels in the infrared. The variable wavelengths were achieved by many of harmonic generation crystals and stimulated Raman, and a dye laser. Combination of all these laser line generating techniques has provided a practically tunable UV to IR laser source. The pump and probe pulses are coincident in the sample. The probe beam alone will be through the sample without change in its intensity because the sample does not absorb at the probe wavelength. However, when heat is generated in the sample after absorption of the pump beam then the intensity of the probe beam changes. The intensity fluctuation of the probe beam was measured by means of a photodetector which consisted of either a photomultiplier or a two dimensional vidicon which is capable of recording the intensity vidicon which is capable recording the intensity and spatial distribution of the beam. The intensity at a given laser power of the pump was recorded from the reading obtained from the lock-in amplifier. The heat generation process may be described by

$$\tau_e = (k_1[M])^{-1} = k_e^{-1}$$

where k_1 is the bimolecular rate constant and k_e is the first rate constant. In the case where heat transfer ion transfer in the same manner as acoustic waves, the transit time across the laser beam is

$$\tau_s = \frac{r_b}{c}$$

were r is the radius of the laser beams, the time for the heat diffusion may then be represented by

$$\tau_d = \frac{r_b^2}{4D_{12}}$$

then the thermal conductivity becomes

$$\tau_{th} = \frac{PC_p r_b^2}{4RTA}$$

If the irradiation by the laser persists for a period of time and the conductivity of the medium is low enough to reach thermal equilibrium then the steady state equilibrium intensity takes the form

$$I = KP\left(\frac{dn}{dt}\right)\frac{A}{dk}$$

where c is a constant with value of μ1.2 the above equation, as well as the previous one make it clear that the sensitivity signal, of thermal lensing depends upon the power as well as the thermo optical properties of the matrix material such as the solvent or encapsulant. The utilization lasers with powerful pulses such as nanosecond or picosecond pulses allows for extreme sensitivity of detection. In fact, several molecules have been identified with absorptivities of the order of 10^{-7}. The materials which we investigated consisted of triphenyl phosphate in acetonitrille, $(CH_3)_2$ CO in CH_3 CN and $CH_3)_2$ SO dissolved in water.They were dissolved in organic solvents such as CH_3CN and n-pentane because these solvents have low thermal conductivity, 1.03 and 1.13 MW cm^{-1} K^{-1} respectively and rather large changes in the index of refraction as a function of temperature(dn/dT); 5.90 and -5.5 K^{-1}. This is to be contracted with water which has thermal conductivity of 6.11 and (dn/dT) of -0.8. We do not intend to suggest that this method is not suitable for water solutions only that the signal, hence sensitivity, is increased in the organic solutions by a factor of 40 for cw lasers. However, with high intensity short pulse, the signal decreases in water only by a factor of ~6. The difference in signal is due to deposition of the heat at a very fast rate, and is detailed by very short probe pulses which has the effect of diminishing the fast thermal conductivity of water.

For the period of time of this report, one year, two types of molecules were studied: 1) C=0 containing molecules, 2) P=0 molecules. In addition we studied the diffusion controlled rate of reaction of anilines and the generation string UV laser light by means of a new highly efficient crystal.

Picosecond Transient Absorption Spectra and Kinetics of Salicylidenaniline

The rate of reaction is a very important parameter because it allows one to determine the time interval necessary to detect the agent before reaction takes place. In addition the metastable species formed their identification and kinetics provide the only reasonable means, to our knowledge , for ascertaining the effect of the molecular agent and its diffusion and reaction through and with a medium.

We selected salicylaniline as the first molecule to study because of the various transformatios which this molecule undergoes,the rrather fast rate of the reaction and its interesting functional groups that are involved in reaction and rearangement.

Using the picosecond time-resolved absorption spectroscopic technique, the transient absorption spectra of salicylidenaniline have been investigated and the room-temperature kinetic data are presented. A possible mechanism of the formation of the photochromic products of salicylidenaniline is proposed.

INTRODUCTION

Salicylidenaniline (SA) **1** and its derivatives are well known photochromic substances, *i.e.* upon irradiation with UV light they form colored products which could be bleached by exposure to visible light. Although a number of investigations exploring their photochromism have been reported [1–10], the data on the spectroscopy and kinetics of the transients involved in the formation of colored products, *via* excited state intramolecular proton transfer, is limited.

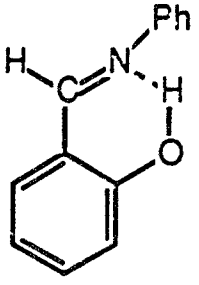

1

Barbara *et al.* [9] presented a detailed study on the fluorescent properties of **1** and its derivatives using time resolved picosecond and nanosecond emission spectroscopy. For the rate of formation of the fluorescing state following the excitation of **1** with a 355 nm laser pulse, they reported a time constant of < 5 ps. At room temperature they observed the fluorescence to decay with a time constant, t_d

= 11 ± 3 ps. At lower temperatures, however, the decay was biexponential consisting of a fast and a slow decay component. The low-temperature fast component (t_d < 5 ps) became too fast to be resolved at room temperature. They assigned the room-temperature single exponential decay, corresponding to the slower component of the low-temperature biexponential decay, to the electronically excited cis-keto tautomer **2** of SA **1**.

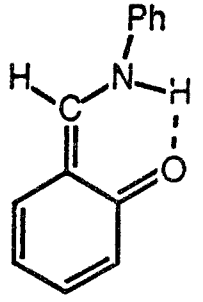

2

Recently, Becker *et al.* [10], using microsecond and nanosecond laser flash photolysis, have reported the absorption spectral data on the transients produced from 355 nm irradiation of SA in various solvents. They assigned the transient absorption spectra with λ_{max} = 460—480 nm (depending on the solvent) to the cis-zwitterion **3** which has previously been reported, by Lewis and Sandorfy [11], as a photoproduct of 365 nm photolysis of **1**.

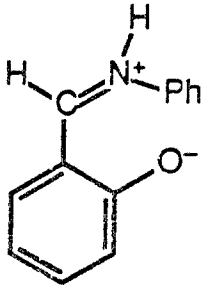

3

For the decay of **3** Becker *et al.* [10] reported a time constant in the microsecond regime, but were unable to assign a specific rise time for the transient **3** due to the 200 ns detection limit of their system.

Inspite of the large amount of research that has been done concerning the photochromicity of SA, the mechanism of the formation of the colored photochromic products from the photolysis of SA is not well established, yet.

The knowledge of the absorption spectra of the transients and their kinetic behavior, especially in the picosecond to nanosecond time domain, is essential in order to obtain a better understanding of the processes leading to the photochromic products of the anils.

To our knowledge, the SA transient absorption spectra and their kinetics in the picosecond regime have not yet been reported. In this report we present the spectral and kinetic data of the transients produced upon the UV excitation of SA in acetonitrile in the picosecond and nanosecond time domain, using the time resolved picosecond laser kinetic-absorption spectroscopic technique.

EXPERIMENTAL TECHNIQUE

The experimental apparatus used in the present investigation have been described in detail elsewhere [12]. Concisely, a single pulse from the output pulse-train (consisting of 9–10 pulses of 30 ps FWHM) of a passively mode-locked Nd:YAG laser was selected. This single beam (l = 1064 nm) after being amplified was split into two, using a beam splitter. One beam was passed through a second- and a third-harmonic crystal, respectively, to generate a 355 nm excitation beam. The other 1064 nm beam was passed through a cell containing a H_2O/D_2O mixture to generate a picosecond continuum which was used to probe any transients formed upon excitation. Time delays between the excitation and the probe beams in the 0 ps to 10 ns range were adjusted using an optical delay stage. Neutral density filters

were used to alternate the probe pulse intensity, and the wavelength region of interest was selected by means of colored optical filters. Data were collected on a vidicon detector, transferred to a personal computer and treated with the appropriate software program.

Each transient spectrum presented in this report represents an average ransient absorption produced by 250 laser pulses. Absorption spectra correspond to the difference in absorbance of the excited and the ground state sample.

For the detection of possible non-linear effects, the transient spectra were recorded as a function of the excitation pulse energy at a fixed time delay between excitation and probe beams. Typically, the excitation beam energy was ~0.3 mJ and the probe beam was focused on the sample in ~1.5 mm diameter.

Salicylidenaniline (minimum purity = 98%) was obtained from Lancaster Synthesis Ltd. and was used as such. The solvent acetonitrile was HPLC grade. All the experiments were carried out at room temperature.

RESULTS AND DISCUSSION

Figure 1 shows the absorption spectrum of the ground state salicylidenaniline in the 300—550 nm region. The time resolved (0 ps—5 ns) absorption spectra, in 425—550 nm region, as obtained following 355 nm excitation of salicylidenaniline are shown in figure 2. From a comparison of the spectra in figure 2 to that in figure 1, it is obvious that the new absorption band in 425—500 nm region does not belong to the ground state SA. Thus it must be due to some new transient species formed upon excitation of SA with the 355 nm laser pulse. As can be seen from figure 2, the absorption intensity exhibits a sharp increase up to 70 ps followed by a slow decrease which levels off at 750 ps after which it goes through another maximum. A comparison of the transient absorption spectra at 25 ps to those at longer times shows a slight red shift (~15 nm) in λ_{max} which may also be seen in figure 2. This

shift is clearly observable by examination of the normalized transient absorption spectra at various times as shown in figure 3 (*e.g.* at 25 ps, 70 ps and 130 ps). From figure 3 it is obvious that the primary transient absorption band (l_{max} ~ 470 nm) disappears with simultaneous growth of the red-shifted secondary absorption band (l_{max} ~ 485 nm). Thus the red-shift in the transient absorption spectra in figure 2 is due to overlap of two different absorption bands. Such spectral behavior indicates that more than one transient species are involved in the formation of photochromic products from 355 nm excitation of SA.

We eliminate the possibility of the generation of the transients being the result of multiphoton absorption because the transient absorbance would then have a non-linear dependence on the excitation pulse energy. Logarithimic plot of the excitation laser pulse energy *vs.* transient absorbance is shown in figure 4. The open circles correspond to the transient absorption intensity (measured at 487 nm) at 75 ps and the solid line is the least mean square fit to the experimental data. Figure 4 exhibits a linear dependence, slope=1, of the transient absorbance *vs* the laser pulse energy in the 0.06–0.39 mJ range.

In order to investigate the kinetic behavior of the transients produced from excitation of the SA with a 355 nm laser pulse, the absorption intensities were plotted as a function of time as shown in figure 5 and 6 for the 0—750 ps and 750 ps—10 ns regions, respectively. For simplicity, all the experimental intensities were normalized to unity. Solid circles are the experimental data *i.e.* the transient absorption intensities obtained from such plots as in figure 2, measured at 487 nm and the solid curve is the computer-generated convolution curve, to fit the experimental data, by a non-linear least square procedure. The time dependence of the transient spectral intensities in 0—750 ps region, as shown in figure 5, exhibits a kinetic behavior involving a single rise (t_{r1}) followed by a biexponential decay (t_{d1}

& t_{d2}). This bimodal decay is followed by a slow rise (t_{r2}) and a slow decay (t_{d3}) as shown by the data in figure 6.

From theoretical fits of the experimental data displayed in figures 5 and 6, we have calculated the following time constants:

1. a very sharp rise, t_{r1} = 18 ps,
2. a biexponential decay of initially formed transient species, with a fast decay component,t_{d1} = 25 ps, and a slow component, t_{d2} = 1.7 ns,
3. a slow rise, t_{r2} = 2.2 ns following t_{d2}, and
4. a slow decay following immediately t_{r2} with a time constant t_{d3} = 3.6 ns after which the transient absorption was found to remain almost constant up to 10 ns—the longest time reached in the present investigation.

On the basis of this kinetic information and the data available in the literature, we assign these time constants to specific transients and thus propose a most probable route for the formation of the photo products resulting from the photolysis of the ground state salicylidenaniline by short laser pulses.

Initial sharp rise time, t_{r1} = 18 ps, indicates a very fast generation of transient species A following the irradiation of SA with a 355 nm laser pulse. Barbara *et al.* [9], based on their picosecond emission spectroscopic studies, have reported a similar time constant (t_{df} ~12 ps) for the fluorescence decay rate after exciting SA in methanol with 355 nm laser pulse at room temperature. They have assigned this fluorescence to the electronically excited cis-quinoid **2** formed *via* intramolecular proton transfer from O to N in the singlet excited state of SA. Recently, Becker *et al.* [10] have also reported a similar time constant, t_{df} < 30 ps (detection limited), for the fluorescence decay of SA in acetonitrile. They further noticed an increase in the fluorescence life time with polarity of the solvent. Thus Barbara *et al.*'s t_{df} would be expected to be > 12 ps in more polar solvents like acetonitrile. Owing to the fairly good agreement between the measured fluorescence decay time, t_{df}, and the

transient absorption rise time, t_{r1}, it is quite reasonable to assume that the ground state of the fluorescence in Barbara *et al.*'s experiments and of the initial transient absorption in the present investigation represent the same species. Thus the primary transient **A** in our picosecond absorption study could be identified as cis-quinoid **2** in its ground state.

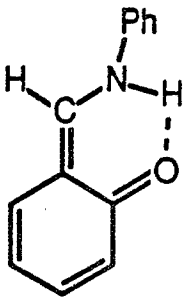

A (cis-quinoid)

Next task is to analyze the observed biexponential decay of the transient absorption as shown in figure 5. A possible explanation for such an observation would be that the transient **A** decays *via* two different paths — a fast one (t_{d1} = 25 ps) and a slow one (t_{d2} = 1.7 ns) as shown in scheme 1.

Scheme 1:

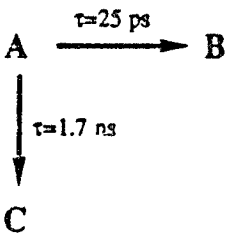

Another possibility is that the observed biexponential decay is actually an overlap between single decays of two different species as shown in scheme 2.

Scheme 2:

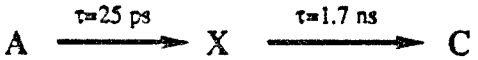

In order to decide between these two possibilities we have to first identify species B and X associated with the fast decay component (t_{d1} = 25 ps).

Since, within experimental error limits, t_{r1} (= 18 ps) and t_{d1} (= 25 ps) are quite similar, we may assume that they probably represent the same process. Also the ground state enol form 1 of SA is more stable than the ground state cis-quinoid, thus it seems appropriate to propose that t_{d1} = 25 ps correspond to the fast decay of A to 1.

$$A \text{ Æ } 1 \qquad\qquad t_{d1} = 25 \text{ ps}$$

Also, upon probing the 355 nm excited sample of SA at 355 nm, a small bleaching of the ground state SA was observed which lasted for < 25 ps. This fast recovery of the ground state of SA further supports the above proposition concerning the fast decay of A (t_{d1} = 25 ps) to 1. The decay of A back to the ground state SA is in agreement with scheme 1 while scheme 2 requires the formation of a new intermediate which undergoes further decay.

Upon analyzing the kinetics of the normalized absorpion bands shown in figure 4, it was observed that the secondary transient absorption band passes through an absorption maximum 70 ps after excitation, with a rise time constant τ'_r = 20 ps. These values of τ'_r and t_{d1} (20 ps and 25 ps respectively) are within experimental error limits and indicates that these two time constants might represent the same process i.e. simultaneous decay of A and formation of a new intermediate. This observation satisfies scheme 2.

Although our observations support the faster (25 ps) step of both schemes 1 & 2, scheme 1 appears to be less probable since t_{d2} is two orders of magnitude slower than t_{d1} and thus would make an insignificant contribution to the decay of A. Thus the observed kinetic behavior for decay of A is better explained by scheme 2. This, however, does not rule out completely the possibility of scheme 1 being also operative at least with a low quantum efficiency. Taking into account these facts, the decay of A can be represented by the following scheme with the dotted arrow representing the least efficient process:

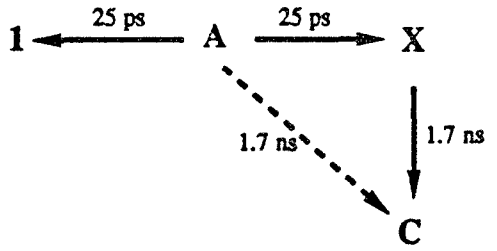

The fast formation of X and its slow decay indicates that X is structurally more close to its parent than its product. We, therefore, propose the following structure to X:

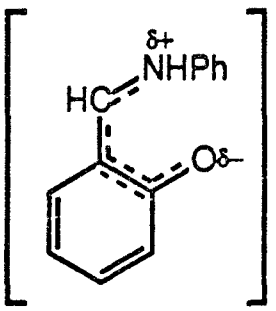

X

The slow decay of the transient absorption (t_{d2} = 1.7 ns) is followed by a slow rise in the transient absorption with a time constant t_{r2} = 2.2 ns. Since the two time constants are similar, within experimenta limit, probably represent the same process.

$$X \text{ Æ } C \qquad\qquad t_{d2} = 1.7 \text{ ns}$$

The slow rate of this process could be due to the different spin states of the two species involved *i.e.* it is a forbidden process. In order to check the presence of any triplet species, crystal violet, a triplet quencher, was added to the system. No change in the kinetic behavior of the transients was observed in the presence of the triplet quencher, which indicates that either there are no triplet species involved or the life time of these triplet species is shorter than the time required for collision with quencher to take place.

Becker *et al.* [10] have reported that based upon nanosecond transient absorption studies on SA, the initial transient is a cis-zwitterion with a rise time in nanosecond region (detection limited). The intermediate **C** in the present work could be this cis-zwitterion.

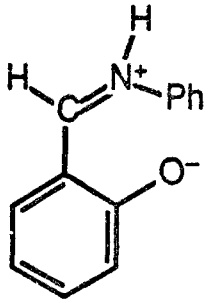

C (cis-zwitterion)

Becker *et al.* [10] reported the time constant for the decay of cis-zwitterion to be 400 ms, whereas from the present study we observed that the cis-zwitterion decays with a time constant of 3.6 ns followed by no further observable decay during the 10 ns period, the upper time limit reached in this investigation. A possible explanation for such kinetic behavior is that the cis-zwitterion follows a bimodal decay consisting of a fast component, t_{d3} = 3.6 ns, and a slow component in the microsenod region corresponding to the almost constant decay up to 10 ns as observed in the present study. Thus the slow component (shown by dashed arrow 2 in the scheme below) of this biexpoenetial decay corresponds to the decay time constant of 400 ms as reported by Becker *et al.* who, probably, were unable to see the fast decay component. Next question is: what is the structure of the intermediate to which cis-zwitterion decays in 3.6 ns? Since ionic species like zwitterion would be stabilized in a polar solvent such as acetonitrile, and because its decay time, t_{d3} = 3.6 ns, is longer than its rise time,t_{r2} = 2.2 ns, the decay of cis-zwitterion would be expected to a non-ionic intermediate, which we tentatively propose to be a trans-

quinoid which subsequently decays very slowly to the final products. This is shown by the dashed arrow 3 in the scheme below.

Based on the present kinetic data and the data available in literature, the most probable mechanism of the photochromic product formation by 355 nm excitation of SA can be represented as follows:

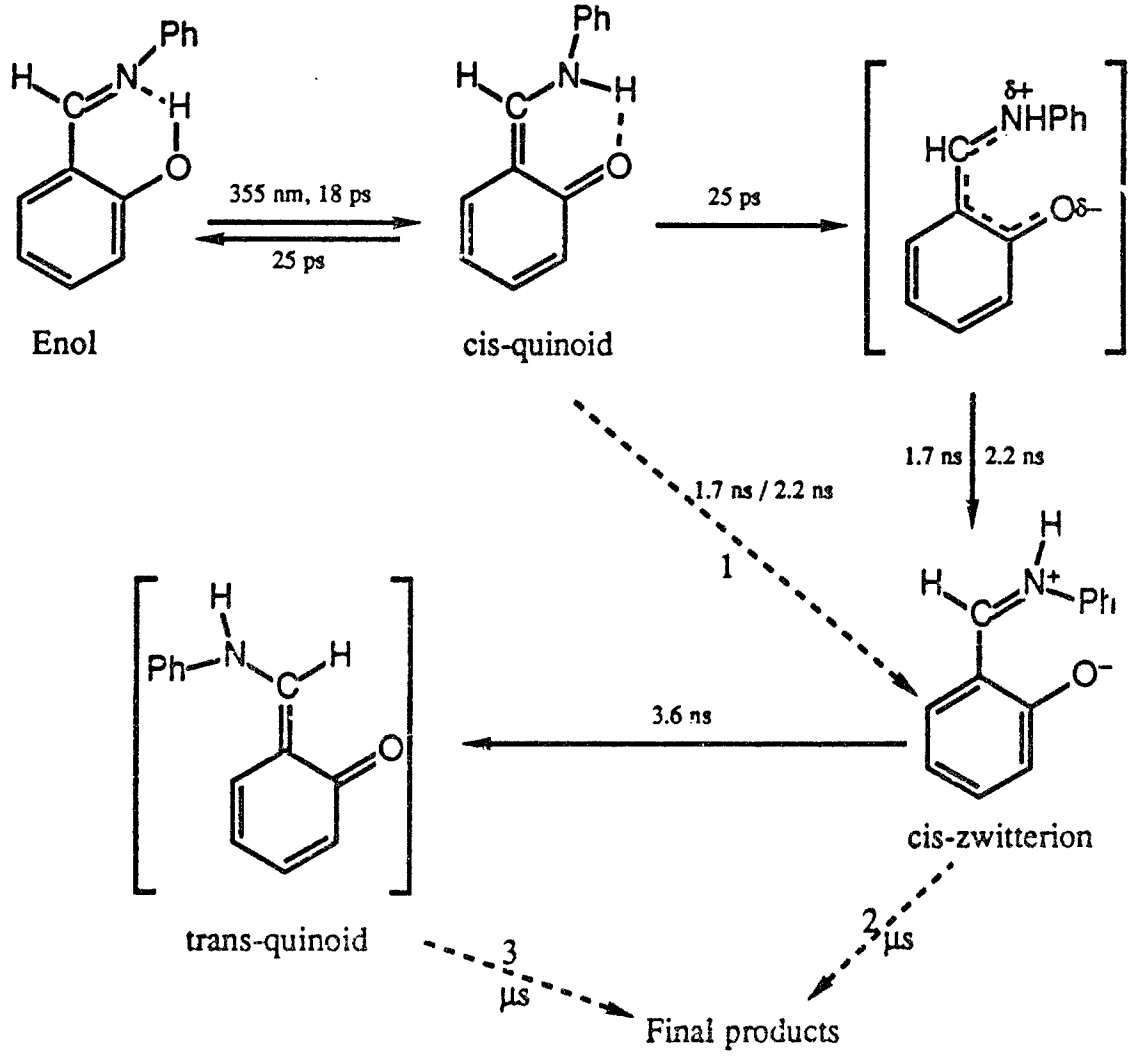

We found that the amount of laser power needed at the UV wavelengths in order to detect 10^{-8} M and lower concentrations should be improved by at least a factor of four under identical conditions of solvent and laser fundamental. Tot his effect we performed the necessary theretical calculations to determine the feasibility of using a new nonlinear crystal, Barium Borate , (BBO), for the generation of high power pulses in the UV. We also performed experiments which prove that high power pulses are possible from this crystal. We describe below these studies which promise to increase the detection and diffusion rate of PO and SO containing molecule by at least a factor of 10.

Thermal Lensing in Triphenylphosphate

The measurements presented here were made by means of the experimental system based on the thermal lens effect. The experiments were performed in triphenylphosphate, $(PhO)_3PO$ dissolved in acetonytrile. These experiments nsuggest the possibility of detecting very small concentrations of molecules containing the -PO functional group using thermal lensing. in addition it is possible to differentiate among the various similar types of molecules and distinguish between the agent and the simulant.

The ground state electronic absorption spectrum of $(PhO)_3PO$ in CH_3CN is shown in figure 7, and the experimental setup for the dual beam thermal lens technique is shown in figure 8. A passively mode-locked pulsed (1Hz) Nd:YAG laser was used as a pump source and a He-Ne laser was used as a probe source. The output from the Nd:YAG laser (1064 nm, 30 ps FWHM) was frequency quadrupled to generate 266 nm pump beam using a 2^{nd} and a 4^{th} harmonic generation, KDP, crystals. Focusing the pump beam through the sample length generated a thermal lens which was then detected by the probe beam from the He-Ne laser following the same path through the sample as the pump beam. A sharp cut filter was used to cut off the pump

beam after the sample cell. The probe beam, after passing through an iris diaphragm, was focused onto the slit of an optical multichannel analyzer (OMA).

Typically 1.0 cm path length cell was used for all the measurements except at very low concentrations in which case a cell of path length 2.0 cm was used. The pump beam energy was in 0.5 to 1 mJ range. For a typical experiment, sample was simultaneously exposed to both the pump and the probe beams, and the probe beam intensity reaching the OMA was collected for 60 pump pulses. This probe beam intensity was corrected for the background noise of the detector and recorded as I_1. Same procedure was repeated while the pump beam was blocked, and the probe beam intensity after being corrected for the background noise was recorded as I_2. The change, $DI=I_2—I_1$, in the probe beam intensity corresponds to the thermal lens effect produced by the pump beam. The above experiment was repeated at various dilutions of the sample untill a minimum concentration was reached where no change in the probe beam intensity could be observed. For each experiment, it was assured that the pump and the probe beam overlapped throughout the sample length. Magnitude of the thermal lens generated by the pump beam was found to be directly proportional to the sample concentration as shown by the linear plot of DI *vs* [triphenyl phosphate], in figure 9.

With this present setup we were able to observe thermal lensing in $(PhO)_3PO$ solutions as dilute as $6x10^{-6}$ moles/litre.

Similar thermal lens experiments were performed on molecules containing -CO and -SO functional groups, e.g. $(CH_3)_2CO$ and $(CH_3)_2SO$. In

both these cases, the minimum concentration at which thermal lensing could be observed was much higher than in case of $(PhO)_3PO$, see Table 1.

However, it is expected that the thermal lens effect could be observed at concentrations lower than micro moles per litre, provided that the pump laser output is stable over a number of pulses, is of high enough enrgy to generate sufficient amount of thermal lensing , and that the detection system is very sensitive to record minute changes in the probe beam intensity due to thermal lensing.

Table 1.

Substance/solvent	Functional group	Minimum concentration at which thermal lensing was observed
$(PhO)_3PO/CH_3CN$	—P=O	6.4×10^{-6} M
$(CH_3)_2CO/CH_3CN$	—C=O	7×10^{-4} M
$(CH_3)_2SO/H_2O$	—S=O	~0.5 M

REFERENCES

(1) Cohen, M.D. and Schmidt, G.M.J. *J. Phys. Chem.* 1962, *66*, 2442.

(2) Anderson, D.G. and Wettermark, G. *J. Am. Chem. Soc.* 1965, *87*, 1433.

(3) Ottolenghi, M. and McClure, D.S. *J. Chem. Phys.* 1967, *46*, 4620.

(4) Becker, R.S. and Richey, W.F. *J. Am. Chem. Soc.* 1967, *89*, 1298.

(5) Richey, W.F. and Becker, R.S. *J. Chem. Phys.* 1968, *49*, 2092.

(6) Potashnik, R. and Ottolenghi, M. *J. Chem. Phys.* **1969**, *51*, 3671.

(7) Rosenfeld, T; Ottolenghi, M and Meyer, A.Y. *Mol. Photochem.*, **1973**, *5*, 39.

(8) Higelin, D. and Sixl, H. *Chem. Phys.* **1983**, *77*, 391.

(9) Barbara, P.F.; Rentzepis, P.M. and Brus, L.E. *J. Am. Chem. Soc.* **1980**, *102*, 2786.

(10) Becker, R.S.; Lenobe, C. and Zein, A. *J. Phys. Chem.* **1987**, *91*, 3509.

(11) Lewis, J.W. and Sandorfy, C. *Can. J. Chem.* **1982**, *60*, 1738.

(12) Guest, C.R.; Straub, K.D. and Rentzepis, P.M. *Res. Chem. Intermed.* **1989**, *12*, 203.

Figure Captions

Figure 1. Ground state absorption spectrum of salicylidinaniline, $4x10^{-4}$ M in acetonitrile, in 300—550 nm region.

Figure 2. Time resolved transient absorption spectra as obtained from the excitation of $4x10^{-4}$ M solution of SA in acetonitrile with 355 nm picosecond laser pulses. Each spectrum represents an average of data collected from 250 laser pulses.

Figure 3. Comparison of the normalized transient absorbance at 70 ps and 130 ps to the transient absorbance at 25 ps. The normalized spectra at 70 ps and 130 ps were obtained by subtracting from the transient absorption spectrum at these times (such as in figure 2) the corresponding spectrum at 25 ps.

Figure 4. Logarithmic plot of the transient absorbance *vs* laser pulse energy. Open circles correspond to the experimental results and the solid line is the least square fit to the experimental data. A slope of unity is observed.

Figure 5. Time dependence of the transient absorbance in the 0—750 ps region. Solid circles represent the experimental results and the solid curve is the theoretical fit to the experimental data and yielded the following time constants for the rise and decay of transient absorbance: t_{r1} = 18 ps, t_{d1} = 25 ps and t_{d2} = 1.7 ns.

Figure 6. Time dependence of the transient absorbance in the 750 ps to 10 ns region. Solid circles represent the experimental results and the solid curve is the theoretical fit to the experimental data and yielded the following time constants for the rise and decay of transient absorbance: t_{r2} = 2.2 ns and t_{d3} = 3.6 ns.

Figure 7. Absorption spectra of trphenyl phosphate

Figure 8. Schematic representation of the dual beam thermal lensing technique

Figure 9. Change in intensity of the probe beam as a function of PO concentration.

Figure 1.

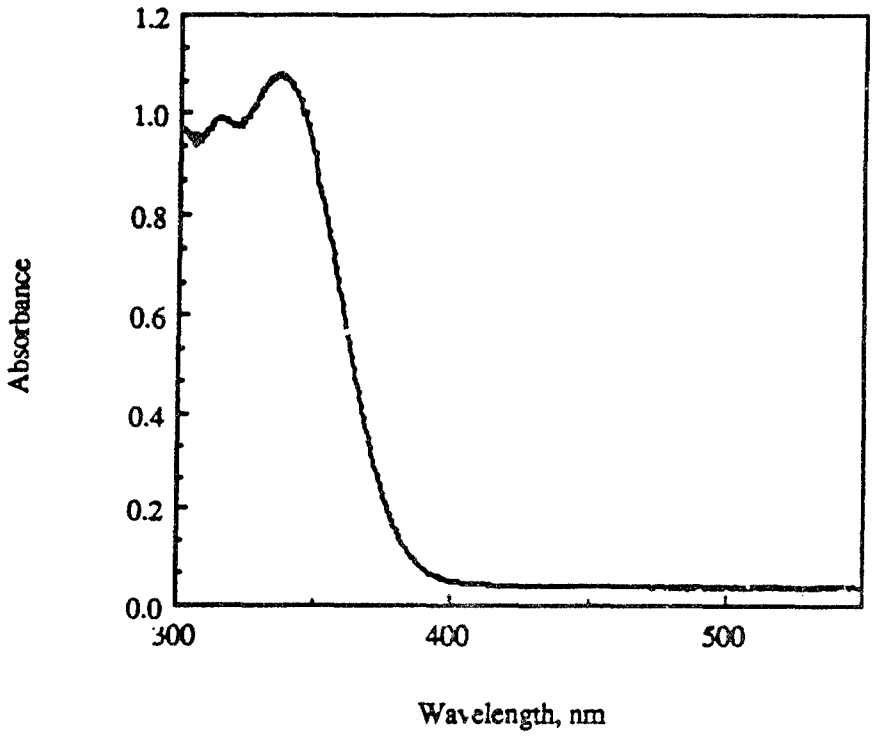

Figure 2.

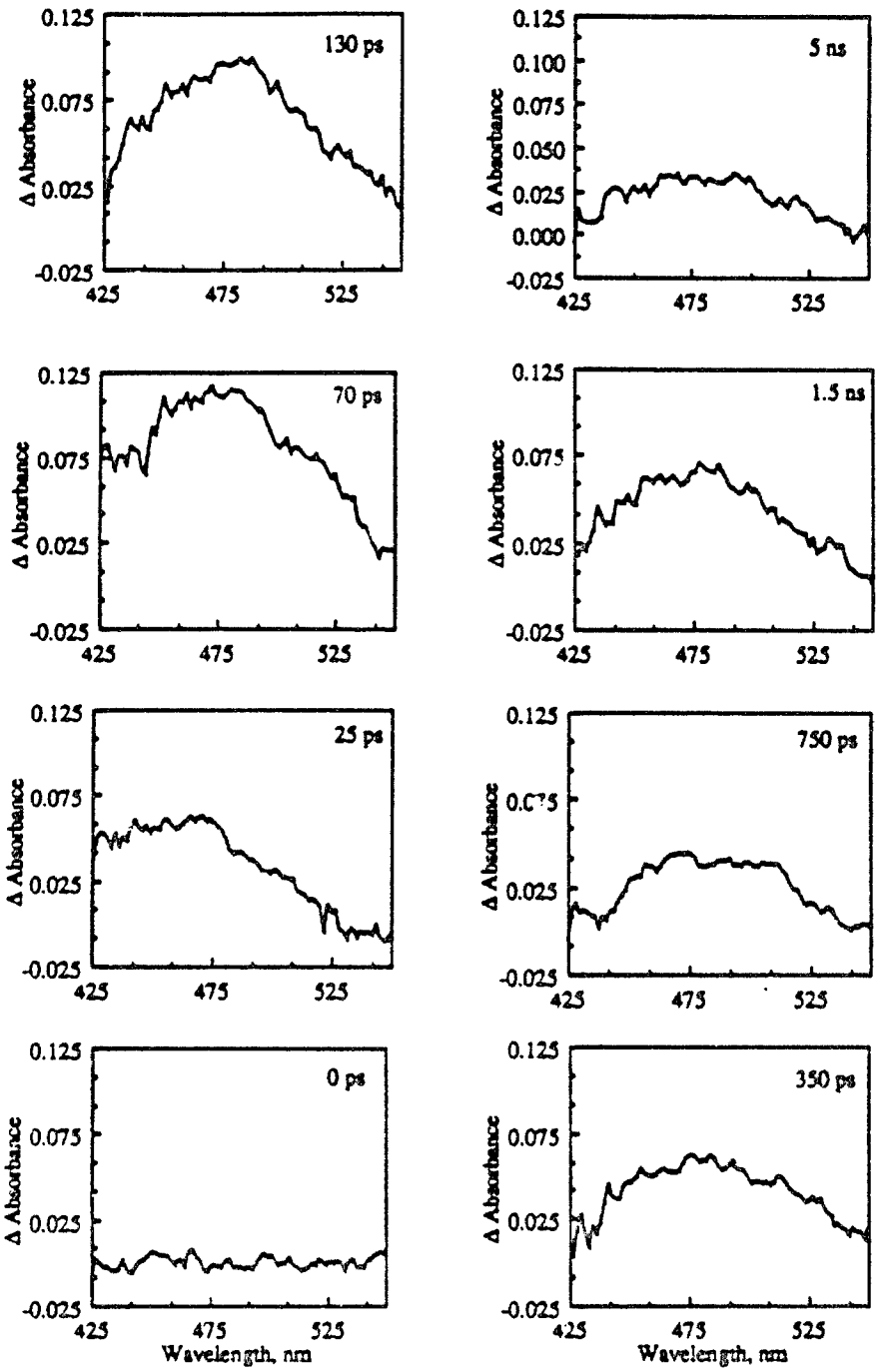
130 ps
5 ns
70 ps
1.5 ns
25 ps
750 ps
0 ps
350 ps
Δ Absorbance
Wavelength, nm
0.125
0.100
0.075
0.050
0.025
0.000
-0.025
425
475
525

Figure 3.

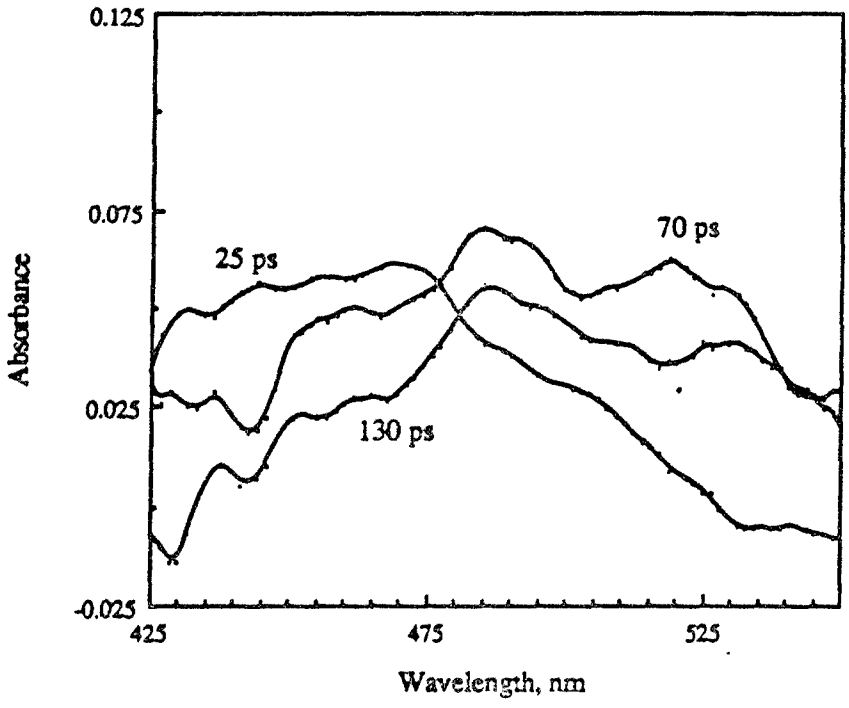
0.125
0.075
0.025
-0.025
Absorbance
25 ps
70 ps
130 ps
425
475
525
Wavelength, nm

Figure 4.

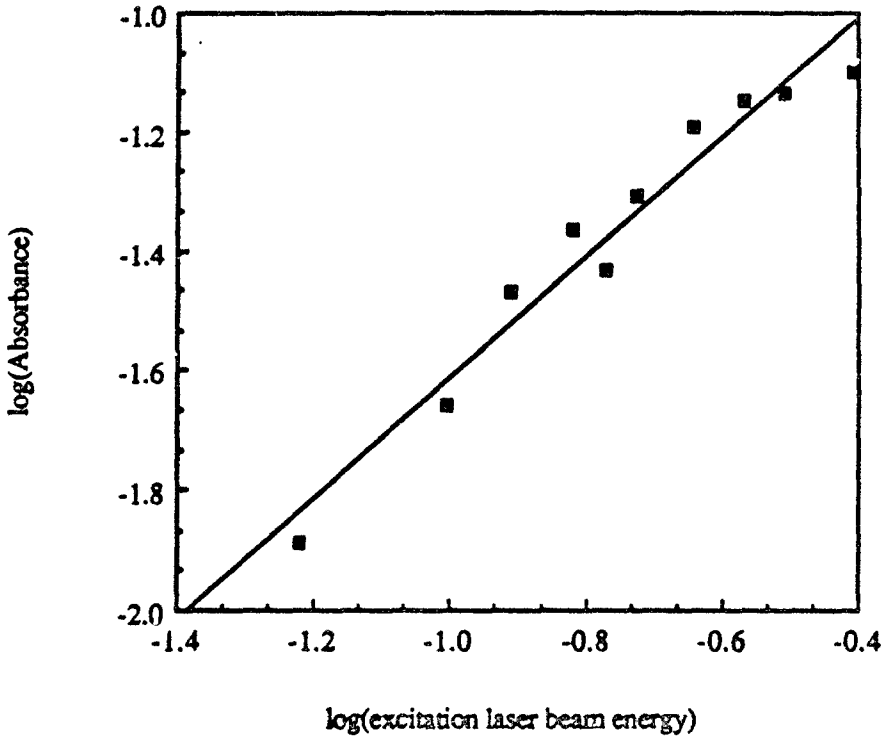
-1.0
-1.2
-1.4
-1.6
-1.8
-2.0
log(Absorbance)
-1.4
-1.2
-1.0
-0.8
-0.6
-0.4
log(excitation laser beam energy)

Figure 5.

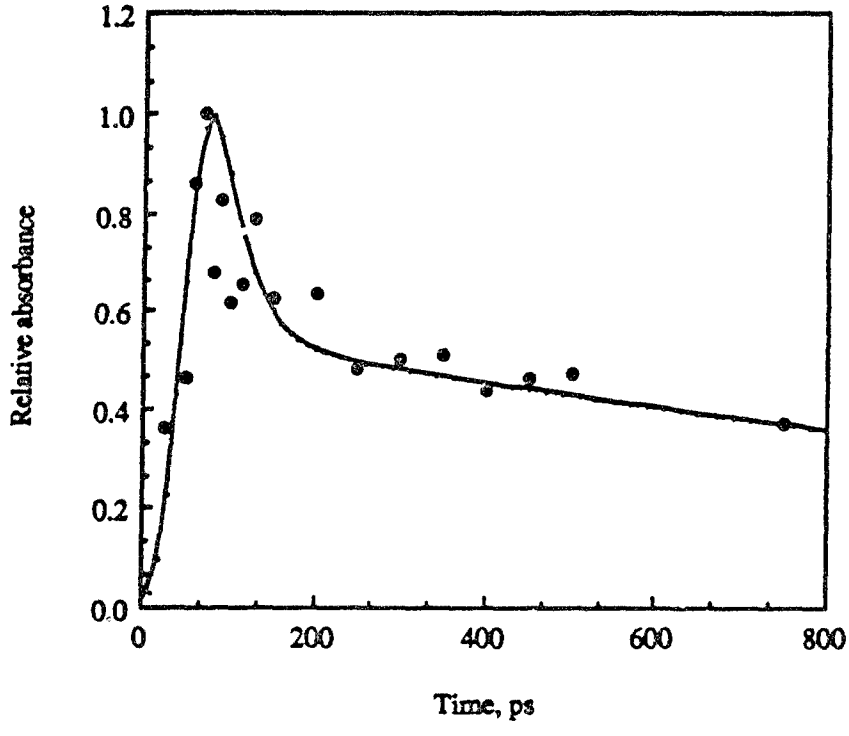
1.2
1.0
0.8
0.6
0.4
0.2
0.0
Relative absorbance
0
200
400
600
800
Time, ps

Figure 6.

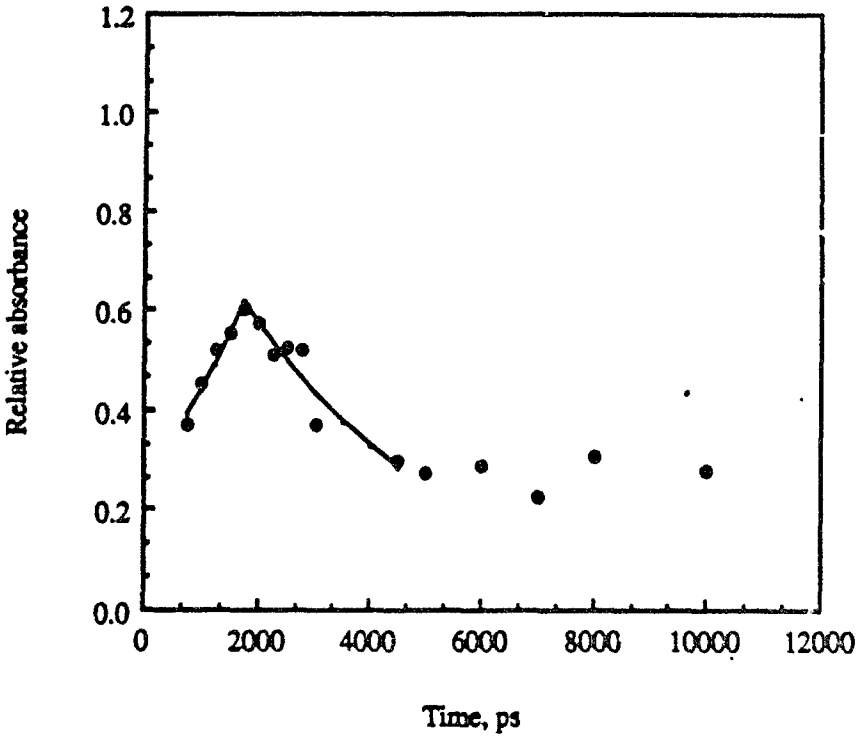
1.2
1.0
0.8
0.6
0.4
0.2
0.0
Relative absorbance
0
2000
4000
6000
8000
10000
12000
Time, ps

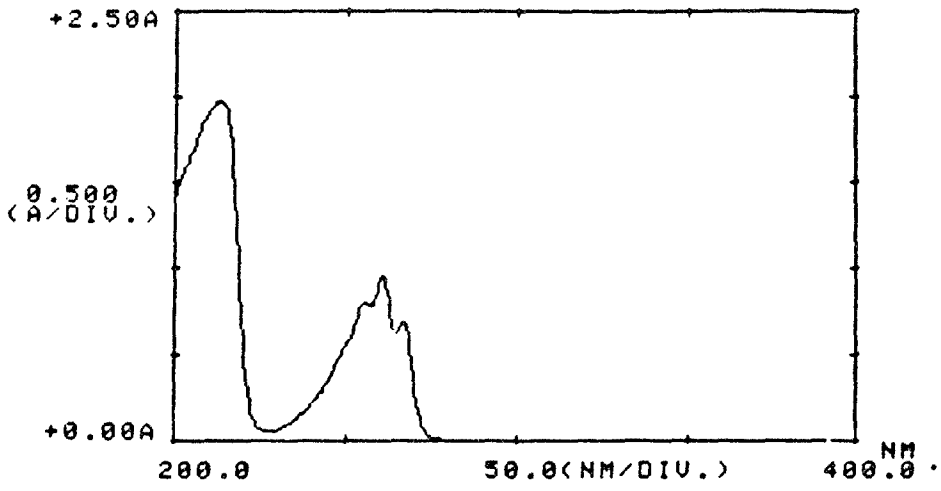
+2.50A
0.500
(A/DIV.)
+0.00A
200.0
50.0(NM/DIV.)
400.0
NM

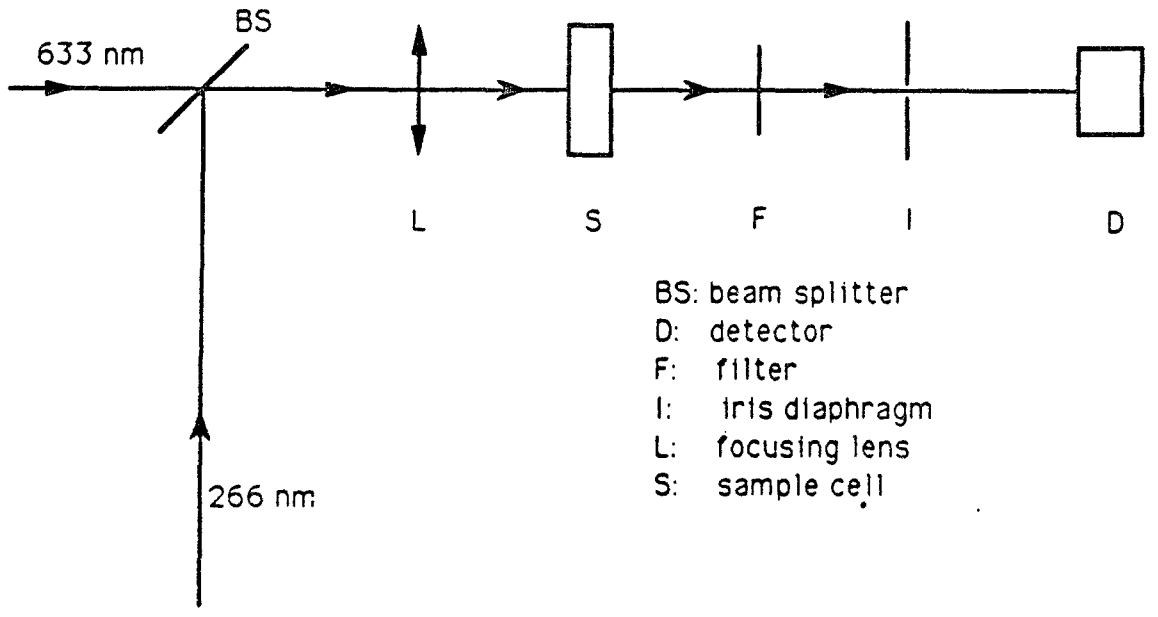

Figure 2: Schematic diagram of the dual beam thermal lens technique.

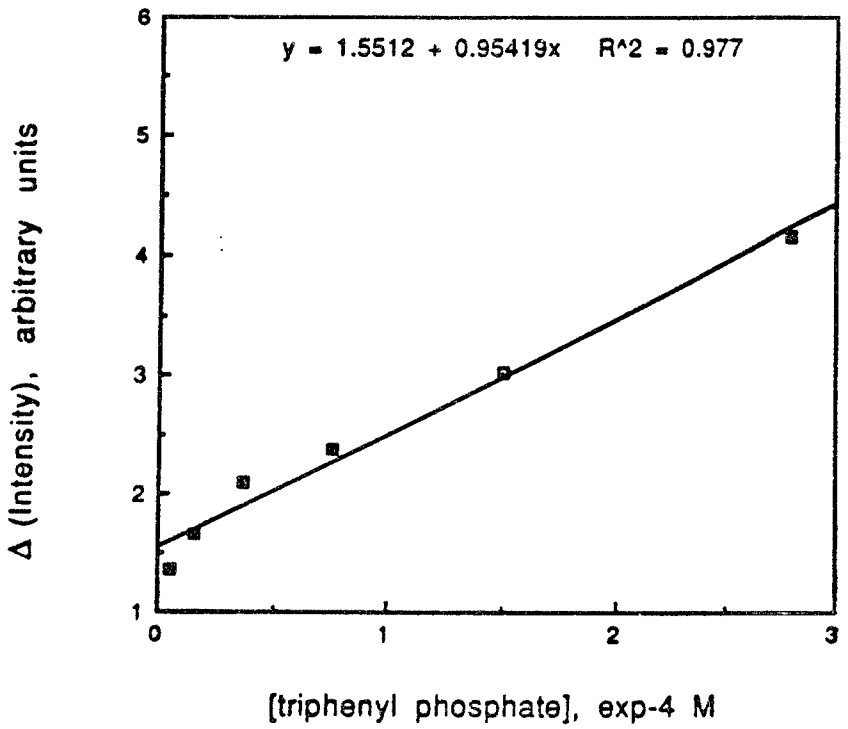
y = 1.5512 + 0.95419x R^2 = 0.977
Δ (Intensity), arbitrary units
[triphenyl phosphate], exp-4 M
1
2
3
4
5
6
0
1
2
3

LIST OF PUBLICATIONS

Picosecond Transient Absorption Spectra and Kinetics of Salicylaniline, V. Sandhu, D. Parthenopoulos, K. D. Straub and P. M. Rentzepis, *J. Res. on Chem. Interme.* **16**, No. 1, 1991

Third Harmonic Generation in Barium Borate, I. V. Tomov, B. Van Wonterghem, P. M. Rentzepis, *Applied Optics* in print.

LIST OF PARTICIPATING SCIENTIFIC PERSONNEL

Tracy F. Dutton (completed Ph.D.)

Dr. Vinod Sandhu

Professor Peter M. Rentzepis